Drop Formation from a Liquid Jet: A Linear One-dimensional Analysis Considered as a Boundary Value Problem

Abstract: Using a one-dimensional model, the author studied drop formation using a boundary value perturbation, rather than a spatially periodic one as considered by Rayleigh. The Rayleigh solution becomes the high jet velocity approximation to this linear analysis. At lower velocities the analysis shows that the medium becomes dispersive, and drop formation characteristics are quite different from that predicted by Rayleigh. In an appendix, the gross momentum balance and flow rate conservation are used to consider drop formation from a stream.

Introduction

In 1878 Lord Rayleigh considered the breakup of an inviscid cylindrical jet into drops [1, 2]. He used a reference system wherein the cylinder of liquid was initially at rest and the perturbation applied was spatially periodic. Under appropriate circumstances, surface tension forces broke the liquid into equally spaced drops. Rayleigh then applied the conclusions to a moving jet of liquid emanating from a nozzle.

In his work on drop formation Rayleigh linearized his equations by assuming the variation of the jet radius to be very small compared to the radius itself. This assumption becomes invalid, of course, as drop separation occurs. Nonetheless, Rayleigh's work has given much insight into the phenomenon of liquid jet breakup.

A one-dimensional model of drop separation has been used for the purpose of better understanding the process [3]. In this model, the variables depend on the axial coordinate of the jet and on time. In using such a model, one assumes that the wavelength of perturbations on the stream is large compared to the radius (see, for example, [4]).

Lee looked at the resulting nonlinear equations avoiding the low amplitude assumption made by Rayleigh [3]. Using numerical methods his results show the formation of satellite droplets as well as the main drops. These satellite droplets, which are formed between the main drops of the stream, are observed experimentally but are not predicted by linear models.

The application of the spatially periodic Rayleigh type solution to a jet emanating from a nozzle is somewhat

artificial. In the spatially periodic solution the unstable perturbations grow with time all along the jet. The nozzle problem, however, is a steady state problem in which the unstable perturbations grow with increasing distance from the nozzle. Keller, Rubinow, and Tu [5] considered this problem as one of temporal periodicity rather than of spacial periodicity. Portig, [6] looked at the problem as a boundary value problem, also using the one-dimensional model.

Considering the problem as a boundary value problem takes into account the interaction of the capillary wave velocity with the velocity of the jet. Rayleigh's solution becomes the high jet velocity limit of this boundary value problem when the capillary velocity can be neglected with respect to the jet velocity.

In this paper, the differential equations for the onedimensional model are presented first. These equations are then applied to the spatially perturbed case as considered by Rayleigh for comparison with his work. The differential equations are next used to solve the boundary value problem. In this solution, the dispersion condition is determined and solved. The solutions permitted by the dispersion equation are used to match boundary conditions resulting in the final solution. Finally, the solution is applied to the stream at the drop separation point to yield an equation for separation distance. Results are compared with the Rayleigh type solution. In the appendix, drop formation is considered using gross momentum balance and flow rate conservation.

148

Differential equations

Lee [3] presented the one-dimensional model of drop separation. The resulting differential equations are

$$r\frac{\partial v}{\partial z} = -2\left(v\frac{\partial r}{\partial z} + \frac{\partial r}{\partial t}\right),$$

$$\frac{\partial v}{\partial t} + v\frac{\partial v}{\partial z} = -\frac{1}{\rho}\frac{\partial P}{\partial z}.$$
(1)

In these equations, r and v are the radius of the stream and the velocity of the liquid, respectively. These two variables are functions of both z and t, the time. The coordinate z is the distance along the jet. The density of the liquid is ρ .

The internal pressure of the jet, P, is also a function of z and t. This pressure, which is caused by surface tension, is given by

$$P = T\left(\frac{1}{R_1} + \frac{1}{R_2}\right),\tag{2}$$

where

$$\frac{1}{R_{1}} = \frac{1}{r[1 + (\partial r/\partial z)^{2}]^{\frac{1}{2}}}$$

$$\frac{1}{R_{2}} = \frac{-(\partial^{2} r/\partial z^{2})}{[1 + (\partial r/\partial z)^{2}]^{\frac{3}{2}}}.$$
(3)

In these equations, T is the liquid's surface tension and R_1 and R_2 are the principal radii of curvature.

Rayleigh solution

The spatially perturbed linear solution to the differential equations was also presented by Lee [3] for comparison with Rayleigh's work. If the initial conditions are specified as

$$r = a; v = \nu_0 \cos(2\pi z/\lambda), \tag{4}$$

then this solution is

$$\delta = (\pi \nu_0 / \mu \lambda) \sin (2\pi z / \lambda) \sinh \mu t,$$

$$v = \nu_0 \cos (2\pi z / \lambda) \cosh \mu t.$$
(5)

The wavelength of the perturbation is λ , and δ is given by

$$r = a(1 + \delta). \tag{6}$$

The dispersion relationship that determines μ is

$$\mu^2 = \frac{T}{2\rho a^3} \left(\frac{2\pi a}{\lambda}\right)^2 \left[1 - \left(\frac{2\pi a}{\lambda}\right)^2\right]. \tag{7}$$

Rayleigh obtained the same solution for the radius versus z and t under cylindrically symmetric conditions. However, his resulting dispersion relationship is given by

$$\mu^{2} = \frac{T}{\rho a^{3}} \left(\frac{2\pi a}{\lambda} \right) \frac{I_{0}'(2\pi a/\lambda)}{I_{0}(2\pi a/\lambda)} \left[1 - \left(\frac{2\pi a}{\lambda} \right)^{2} \right], \tag{8}$$

where I_0 is the zero-order hyperbolic Bessel function and I_0 ' is its derivative. Equation (7) is an approximation of Rayleigh's Eq. (8) and can be obtained by expanding the hyperbolic Bessel functions into Maclaurin's series and using the first terms. Lee's Fig. 2 [3] shows values of μ versus λ divided by initial stream diameter using both Eqs. (7) and (8). Comparison of these two equations shows that the one-dimensional model yields results equivalent to those of Rayleigh's work.

For values of λ , the wavelength, greater than the initial circumference of the jet, μ is real and the perturbing disturbance on the jet grows in an exponential fashion. Drop formation eventually occurs. However, if the wavelength of the disturbance is less than the initial circumference of the jet, μ becomes imaginary, and the hyperbolic functions in Eq. (5) become circular functions. In other words, the jet is in the condition of stable oscillation with regard to these shorter wavelength perturbations.

One can arrive at the physical reason for Rayleigh's conclusions by considering the saddle point on the jet surface. When the wavelength of the perturbation equals the initial circumference of the jet, the two principal radii of curvature at the saddle point are equal in magnitude but opposite in direction. For longer wavelengths the principal radius of curvature tending to pinch off the jet predominates. However, for shorter wavelengths the other radius of curvature, which tends to restore the initial jet shape, is larger.

One may use Eqs. (5) and (7) to obtain information about an actual jet having a velocity v_0 and emanating from a nozzle at x equals zero. The situation at a distance x from the nozzle can be discerned by looking at the spatially periodic solution at a time $t = x/v_0$. In order to obtain the time dependence at this point on the jet, one should look at the stationary solution of Eq. (5) while he is moving with a velocity of $-v_0$. In addition, one must include a phase difference that depends upon the distance from the nozzle to the point under consideration; therefore,

$$\delta = -\frac{\pi \nu_0}{\mu \lambda} \sinh \frac{\mu x}{\nu_0} \sin \left(2\pi f t' - \frac{2\pi x}{\lambda} \right),$$

$$v = \nu_0 \cosh \frac{\mu x}{\nu_0} \cos \left(2\pi f t' - \frac{2\pi x}{\lambda} \right),$$
(9)

where

$$f = \frac{v_0}{\lambda}, \ x = v_0 t. \tag{10}$$

Boundary value problem solution

Into Eqs. (1, 2, and 3), make the following substitutions:

$$r = a(1 + \delta), \qquad z = a\xi,$$

$$v = v_0(1+u), \qquad t = \frac{a}{v_0}\tau,$$
 (11)

where a is again the initial radius and v_0 is the jet velocity. If we linearize the equations by assuming δ and u to be small, we obtain

$$\frac{\partial u}{\partial \xi} = -2 \left(\frac{\partial \delta}{\partial \xi} + \frac{\partial \delta}{\partial \tau} \right),$$

$$\frac{\partial u}{\partial \tau} + \frac{\partial u}{\partial \xi} = 2\epsilon^2 \left(\frac{\partial \delta}{\partial \xi} + \frac{\partial^3 \delta}{\partial \xi^3} \right),\tag{12}$$

where

$$\epsilon^2 = \frac{T}{2\rho a v_0^2}. (13)$$

The constant ϵ is associated with the capillary velocity on the jet. This capillary velocity at which transverse waves of small amplitude travel along the cylinder of liquid in a manner analogous to transverse waves on a string is given by

$$v_c = \sqrt{\frac{T}{\rho a}}. (14)$$

It can be seen from this that ϵ is a function of the ratio of the velocity of the jet to its capillary velocity; thus,

$$\epsilon^2 = \frac{1}{2} \frac{v_{\rm c}^2}{v_{\rm o}^2}.\tag{15}$$

Assume the following steady state solution for Eq. (12):

$$u = u_0 e^{i(\omega \tau - \kappa \xi)}$$

$$\delta = \delta_0 e^{i(\omega \tau - \kappa \xi)}, \tag{16}$$

where ω is a real constant but κ is a constant that can assume complex values. By substituting Eq. (16) into Eq. (12) one obtains

$$-\kappa u_0 + 2(\omega - \kappa) \delta_0 = 0$$

$$(\omega - \kappa)u_0 - 2\epsilon^2 \kappa(\kappa^2 - 1) \delta_0 = 0. \tag{17}$$

In order for nontrivial solutions to occur, the determinant of Eq. (17) must equal zero; the following dispersion relationship results:

$$\epsilon^2 \kappa^4 - (1 + \epsilon^2) \kappa^2 + 2\omega \kappa - \omega^2 = 0. \tag{18}$$

The coefficient of the time variable is normally the angular frequency; however, a substitution for t, the time, was made. From the definition of τ , Eq. (11), one can say

$$2\pi f = \frac{v_0 \omega}{a} = \frac{2\pi v_0}{\lambda_0}.$$
 (19)

Therefore,

$$\omega = \frac{2\pi a}{\lambda_0} = \frac{\pi}{\lambda_0/d}.$$
 (20)

Thus one can see that ω is the same constant that was encountered in Eqs. (7) and (8). Because the problem is restricted to positive values of v_{o} , only positive values of ω are of interest.

Roots of the dispersion equation

In order to help examine the roots of Eq. (18), the following polynomial is defined:

$$p(\kappa) = \epsilon^2 \kappa^4 - (1 + \epsilon^2) \kappa^2 + 2\omega \kappa - \omega^2. \tag{21}$$

This is a fourth-order polynomial with real coefficients. It, therefore, has four roots, in general, and if complex roots exist, they must occur in conjugate pairs.

Two of the roots of Eq. (21) must be real. This can be seen by noting that p becomes positive for large values of κ and is negative for κ equal to zero or one. The curve must, therefore, cross the p=0 axis. As it turns out, there are regions of ω and ϵ where four real roots exist and where two real roots and two complex roots exist.

Let us find the boundary between the regions where four distinct real roots exist for Eq. (18) and where two complex roots occur (at this boundary, a double real root exists). Therefore, the quadratic factor made of this double root must divide into p (Eq. (21)) leaving another quadratic factor with no remainder terms; therefore,

$$\frac{p(\kappa)}{(\kappa - \gamma_{\rm D})^2} = \text{quadratic},\tag{22}$$

where $\gamma_{\rm D}$ is the double root.

By performing the division of Eq. (22) and setting the two remainder terms equal to zero, one can obtain:

$$\gamma_{\rm D} = \frac{\omega}{2(1+\epsilon^2)} (3 \pm \sqrt{1-8\epsilon^2}),$$

$$2\epsilon^2 \gamma_{\rm p}^3 - (1 + \epsilon^2) \gamma_{\rm p} + \omega = 0. \tag{23}$$

These two equations can also be obtained by noting that, at a double root, not only must p (Eq. (21)) equal zero, but its derivative with respect to κ must equal zero

The following boundary relationship can be obtained from Eq. (23):

$$\omega^{2} = \frac{1}{32\epsilon^{2}} \left[1 + 20\epsilon^{2} - 8\epsilon^{4} \pm (1 - 8\epsilon^{2})^{\frac{3}{2}} \right]. \tag{24}$$

Figure 1 shows the boundaries delineated by the equation as well as the regions where the various types of roots occur. The region where complex roots exist cor-

responds to the case of unstable equilibrium of the cylindrical jet, where the perturbations grow and drop formation takes place. The region where only real roots occur yields the case of stable equilibrium where no drop formation takes place.

The Rayleigh solution involves the approximation for which the jet velocity is much greater than the capillary velocity. This approximation is given by letting ϵ approach zero. If one looks at Fig. 1 along the y axis ($\epsilon^2 = 0$), he will note the same conclusions made by Rayleigh. If ω is less than one (see Eq. (20)), drop formation occurs. For ω greater than one, stable equilibrium of the jet exists. With this figure, however, a major departure from the Rayleigh solution is noted. The regions of drop formation are much larger than predicted by Rayleigh and, at lower jet velocities, encompass all wavelengths of disturbance.

Figure 1 also shows a "forbidden zone" delineated by a dashed line. This zone, given by considerations not included in this linear analysis, is discussed in the Appendix.

Solution of the dispersion equation

Note that the cubic term is missing in Eq. (18). With this, one can express the four solutions to this dispersion equation as

$$\kappa_1 = \gamma + i\sigma,$$
 $\kappa_2 = \gamma - i\sigma,$
 $\kappa_3 = -\gamma + \beta,$

$$\kappa_4 = -\gamma - \beta, \tag{25}$$

where γ and β are real constants. By reforming the fourth-order polynomial from the four solutions and equating terms with those of Eq. (18), we have

$$\sigma^{2} = \frac{\omega}{2\gamma\epsilon^{2}} + \left[\gamma^{2} - \frac{(1+\epsilon^{2})}{2\epsilon^{2}}\right],$$

$$\beta^{2} = \frac{\omega}{2\gamma\epsilon^{2}} - \left[\gamma^{2} - \frac{(1+\epsilon^{2})}{2\epsilon^{2}}\right],$$
(26)

$$4\epsilon^{4} \gamma^{6} - 2\epsilon^{2} (1 + \epsilon^{2})\gamma^{4}$$

$$+ \left[\frac{1}{4} (1 + \epsilon^{2})^{2} + \omega^{2} \epsilon^{2}\right] \gamma^{2} - \frac{\omega^{2}}{4} = 0.$$
(27)

The fourth-order equation is, therefore, transformed into a cubic one. These equations may be used to determine the four solutions.

As stated before, the Rayleigh solution corresponds to the boundary value problem solution when ϵ goes to zero as a limit. Therefore, let us expand γ in the Maclaurin series about $\epsilon^2 = 0$:

$$\gamma^2 = \omega^2 \sum_{i=0}^{\infty} b_j \epsilon^{2j}. \tag{28}$$

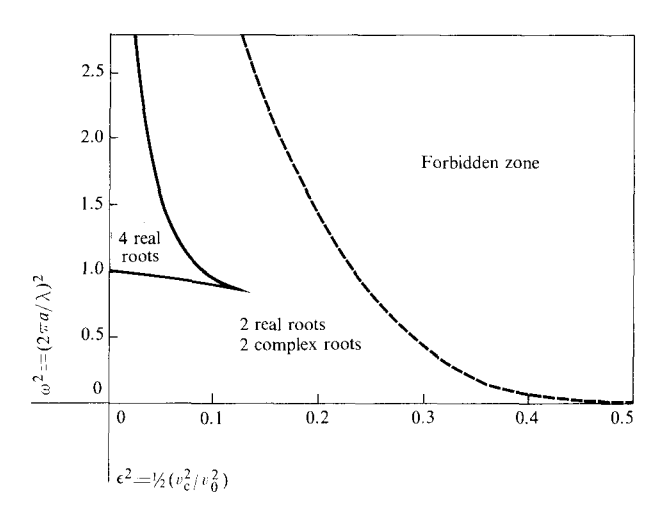


Figure 1 Regions containing different roots of the dispersion equation, Eq. (18), and forbidden zone of drop formation.

Using Eq. (27) to find the derivatives of γ at ϵ^2 equal to zero, one can determine the first three coefficients as

$$b_0 = 1$$
 $b_1 = 4\omega^2 - 2$
 $b_2 = 32\omega^4 - 24\omega^2 + 3.$ (29)

After substituting this series into Eq. (26), we obtain

$$\sigma^2 \approx \omega^2 \epsilon^2 (1 - \omega^2),$$

$$\beta^2 \approx (1/\epsilon^2) \left[1 + (1 - 2\omega^2) \epsilon^2 \right].$$
 (30)

Recapitulating, the first-order solution of the dispersion relationship as ϵ^2 goes to zero is given by

$$\gamma_0 \approx \omega,$$

$$\sigma_0 \approx \omega \epsilon \sqrt{1 - \omega^2},$$

$$\beta_0 \approx \frac{1}{\epsilon}.$$
(31)

Comparing these first-order values with Eqs. (7) and (9), we find that γ_0 and σ_0 compare with the Rayleigh coefficients as

$$\gamma_0 = \frac{2\pi a}{\lambda},$$

$$\sigma_0 = \frac{a}{v_0} \mu.$$
(32)

In the present problem γ is then associated with the wavelength of the disturbance on the jet, and σ is the instability factor that controls the rate at which drop formation occurs. The constant β is associated with the two solutions that do not appear in the Rayleigh solution.

Figure 2 shows the instability factor σ as a function of the relative wavelength for a number of jet velocities. The values were calculated using Eqs. (26) and (27),

151

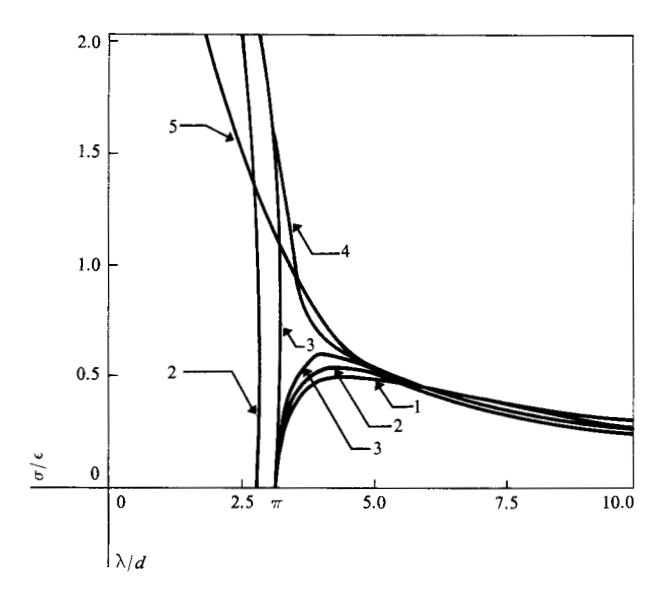


Figure 2 Normalized instability growth factor for the jet velocities indicated in Table 1. Curve 1 is from Eq. (7); other curves are from Eq. (26).

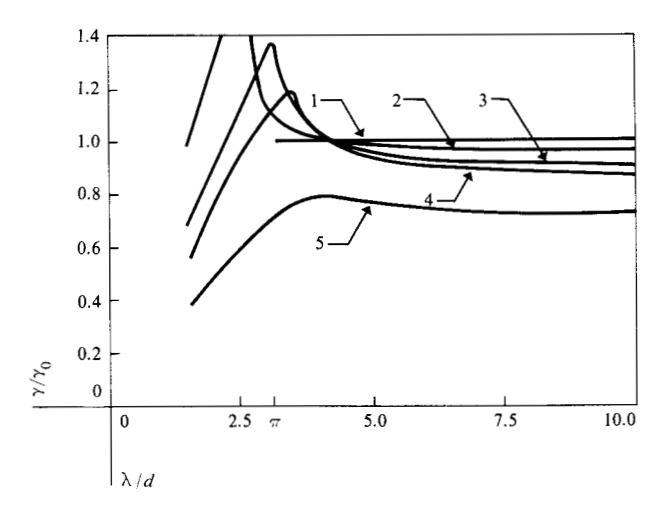


Figure 3 Normalized propagation constant for the jet velocities in Table 1. Curves 2 through 5 are from Eq. (27), λ_0 from Eq. (32)

Table 1 Data used in Fig. 2 through 5.

| Curve no. | | $v_{ m o}/v_{ m c}$ |
|-----------|--------------------------------------|---------------------|
| 1 | (Rayleigh type) | |
| 2 | (Rayleigh type) $\epsilon^2 = 0.060$ | 2.89 |
| 3 | = 0.125 | 2.00 |
| 4 | = 0.175 | 1.69 |
| 5 | = 0.400 | 1.12 |
| | | |

and values are shown only in that region where σ is real. Note that the maximum of the instability factor shifts to shorter wavelength disturbances at lower jet velocities.

Figures 3 and 4 show γ and β relative to their first-order values as functions of the relative wavelength for the jet velocities shown in Table 1. Here again the values were calculated using Eqs. (26) and (27). The nonzero slope of the propagation constant curves indicate the "propagating medium" to be dispersive. The medium is normally dispersive in the region where the slope of Fig. 3 is negative; the dispersion is anomalous where the slope is positive.

Boundary conditions

At z equals zero, where the jet emanates from the nozzle, the following boundary values exist:

$$r = a$$
,

$$\frac{\partial r}{\partial z} = 0,$$

$$\frac{\partial^2 r}{\partial z^2} = 0,$$

$$v = v_0 + \nu_0 \cos 2\pi f t. {(33)}$$

The second boundary equation exists because the liquid cannot make a finite change in velocity in an infinitesimal distance without an infinite force applied. (It should be remembered that with an inviscid liquid, the velocity profile at the nozzle is flat.) The validity of the third equation can be seen from Eqs. (2) and (3); the pressure must be continuous at z=0 at that point. The last boundary equation is, of course, the applied perturbation.

After substituting the values from Eq. (11) into Eq. (33), the boundary value equations take the form:

$$\delta = \frac{\partial \delta}{\partial \xi} = \frac{\partial^2 \delta}{\partial \xi^2} = 0, \qquad u = \frac{\nu_0}{\nu_0} \cos \omega \tau. \tag{34}$$

The solution to this linear problem is the sum of solutions of the type given by Eqs. (16) with the coefficients chosen to conform to the boundary conditions. Therefore, let

$$\delta = \sum_{j=1}^{4} C_j \kappa_j \cos \Theta_j \text{ and}$$

$$u = \sum_{j=1}^{4} d_j \cos \Theta_j,$$
(35)

where:

$$\Theta = \omega \tau - \kappa_i \xi. \tag{36}$$

Upon substituting Eq. (35) into the continuity equation, the first Eq. (12), we obtain

$$\left[\sum_{j=1}^{4} d_{j} \kappa_{j} \sin \Theta_{j}\right] + \left[2 \sum_{j=1}^{4} C_{j} \kappa_{j}^{2} \sin \Theta_{j}\right]$$
$$-\left[2 \sum_{j=1}^{4} \omega C_{j} \kappa_{j} \sin \Theta_{j}\right] = 0. \tag{37}$$

This equation is in the nature of an identity that must be true for all τ and for all positive ξ . Therefore, the coefficient for each Θ_i must add to zero. Therefore,

$$d_i = 2C_i(\omega - \kappa_i). \tag{38}$$

By substituting the first three boundary equations into the first of Eq. (35), we have

$$\begin{split} &\sum_{j=1}^{4} C_{j} \; \kappa_{j} = 0, \\ &\sum_{j=1}^{4} C_{j} \; \kappa_{j}^{2} = 0, \\ &\sum_{j=1}^{4} C_{j} \; \kappa_{j}^{3} = 0. \end{split} \tag{39}$$

In a like manner, substituting the last boundary equation into the second of Eq. (35), we obtain

$$\frac{\nu_0}{\nu_0}\cos\omega\tau = 2\sum_{i=1}^4 C_j (\omega - \kappa_j)\cos\omega\tau \tag{40}$$

or

$$\sum_{j=1}^{4} C_j = \frac{\nu_0}{2\omega v_0}.$$
 (41)

Recapitulating from Eqs. (39) and (41):

$$\begin{vmatrix} 1 & 1 & 1 & 1 \\ \kappa_{1} & \kappa_{2} & \kappa_{3} & \kappa_{4} \\ \kappa_{1}^{2} & \kappa_{2}^{2} & \kappa_{3}^{2} & \kappa_{4}^{2} \\ \kappa_{1}^{3} & \kappa_{2}^{3} & \kappa_{3}^{3} & \kappa_{3}^{3} & \kappa_{4}^{3} \end{vmatrix} = \frac{\nu_{0}}{C_{3}} \begin{vmatrix} 1 \\ 0 \\ 0 \\ 0 \end{vmatrix}.$$
 (42)

Lew [7] pointed out the possibility of bringing the matrix Eq. (42) to its symmetric form by using the choice of coefficients in Eq. (35). The matrix in the system of equations is a Vandermande matrix [8]. The analytical solution to Eq. (42), which is also due to Lew, is

$$C_{j} = \frac{\nu_{0}\omega/4\nu_{0}}{(1+\epsilon^{2})\kappa_{i}^{2} - 3\omega\kappa_{i} + 2\omega^{2}}.$$
(43)

The solution to the problem, Eqs. (35), (36), (38), and (43), is in complex form. However, this solution is real. Because κ_3 and κ_4 are real, the third and fourth terms of the solution are real. Because κ_1 and κ_2 are complex conjugates of one another, C_1 and C_2 ; Θ_1 and Θ_2 ; and d_1 and d_2 form conjugate pairs. The sum of the first two terms of the solution is therefore real.

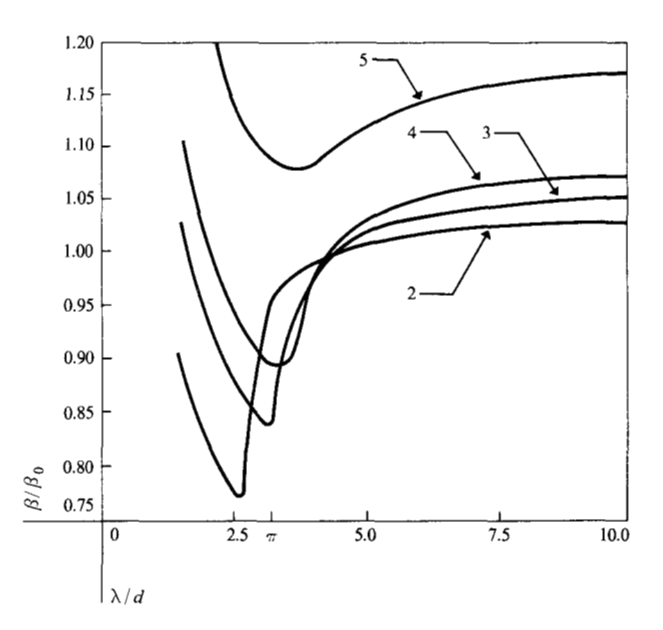


Figure 4 Relative value of the constant β for the jet velocities in Table 1. Curves are from Eq. (26). Because the constant β does not occur in the Rayleigh type solution, Curve 1 does not exist.

It can be shown that the solution approaches the Rayleigh solution, Eqs. (9), as ϵ approaches zero. Equations (25) and (31) give the asymptotic expressions for the four κ terms for this proof.

Drop separation

The point of drop separation can be discerned by looking at the envelope of the radial solution of Eq. (35). One finds the point at which the envelope becomes equal to one, i.e., where the perturbation becomes equal to the original radius. (It must be realized that permitting the perturbation to attain such a value violates the approximations that were made to linearize the original differential equations. So, as with Rayleigh's work, the results obtained from this procedure must be viewed with caution.)

The radial solution consists of the exponentially growing part (the first two terms) and the nongrowing part (the last two terms). By recognizing the assumption that the initial perturbation is very small, the nongrowing part of the solution can be ignored at the break-off point. The first two terms of the radial solution, Eq. (35), can be written

$$\delta = \sqrt{C_1 \kappa_1 C_1^* \kappa_1^*} \left[e^{\sigma \xi} \cos \left(\omega \tau - \gamma \xi + \phi_1 \right) + e^{-\sigma \xi} \cos \left(\omega \tau - \gamma \xi - \phi_1 \right) \right], \tag{44}$$

where

$$\phi_1 = \arctan \left[\frac{(C_1 \kappa_1)_{1m}}{(C_1 \kappa_1)_{2m}} \right]. \tag{45}$$

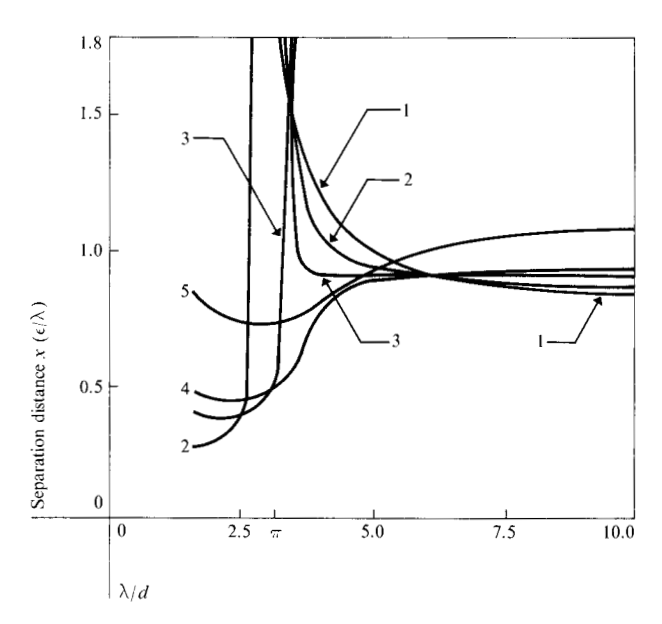


Figure 5 Separation distance normalized with respect to both λ and ϵ for the jet velocities in Table 1. Ratio ν_0/ν_0 equals 0.018. Curve 1 is from Eq. (47); other curves are from Eq. (46).

Of course, the second term in this expression can be ignored at the point of drop separation. Therefore, the envelope to the solution for δ near drop separation is given by

$$\operatorname{Env} = \sqrt{C_1 \kappa_1 C_1^* \kappa_1^*} e^{\sigma \xi}. \tag{46}$$

In a similar way the separation distance as predicted by the Rayleigh solution can be obtained by looking at the envelope. From Eq. (9), the Rayleigh envelope can be given as

$$\operatorname{Env}_{0} = \frac{\omega \nu_{0}}{4 \nu_{0} \sigma_{0}} e^{\sigma_{0} \xi}, \tag{47}$$

where σ_0 is given by Eq. (31).

Figure 5 shows the results. The separation distance (normalized by multiplying by ϵ/λ) is given for a typical value of the initial perturbation. The data for the Rayleightype curve, 1, was obtained from Eq. (47). One can see that the resulting separation distances differ markedly from Rayleigh's results for the lower jet velocities and, of course, for those lower wavelengths where Rayleigh's theory predicts no drop formation.

Conclusions

The one-dimensional model of drop formation has been presented and used again to study the formation of drops in a stream emanating from an orifice. The problem was considered as a boundary value problem wherein a time varying perturbation is placed on the axial velocity at the exit of the orifice. Suitable approximations were made so that the problem could be made linear.

In the boundary-value solution, the Rayleigh solution becomes the asymptotic solution as the jet velocity approaches large values compared to the capillary velocity. The results at such large jet velocities agree with those of Rayleigh. At lower velocities, however, significant differences occur.

The first conclusion that one sees concerns the region of permitted drop formation. At large jet velocities, only perturbations that have a wavelength greater than the initial jet circumference will grow to form drops. At lower jet velocities, growth of the lower wavelength perturbations becomes possible. At jet velocities equal to or less than twice the capillary velocity, drop formation is predicted at any perturbing frequency.

As with Rayleigh's results, the instability factor curve has a maximum for a λ/d ratio of about 4.5 at the high jet velocity limit. At lower velocities, the maximum moves to lower wavelengths and then disappears entirely.

Perhaps the most important observation is that the medium for the wave propagation becomes dispersive. For large jet velocities, and for perturbing wavelengths greater than the initial circumference of the jet, the dispersion of the medium is moderate and normal. For the lower jet velocities and perturbing wavelengths, however, the dispersion becomes more severe and anomalous.

Two additional solutions appear in this boundary value problem. They are associated with the two real roots of the dispersion equation. These two solutions are nongrowing traveling waves, one traveling in each direction, with the forward traveling wave having the higher velocity. The amplitude of these waves goes to zero as the jet velocity becomes large. These solutions, which do not affect the drop formation appreciably in this linear theory, are caused by the dispersive nature of the medium.

The drop separation distances predicted by the analysis are markedly different from those predicted by the Rayleigh solution at lower jet velocities. For lower wavelength perturbations, the separation distance is much less than that predicted by Rayleigh. At longer wavelengths, however, the separation distance becomes greater than the Rayleigh prediction.

It is essential to review the results of the analysis in the light of the approximations made. The one-dimensional model assumes that the wave length is significantly greater than the jet radius. To linearize the equations, the amplitude of the radial and velocity oscillations were assumed to be small compared to the radius and to the capillary and jet velocities. Therefore, in the range of small wavelengths and small jet velocities, the results should be viewed with some caution. As an example, the gross momentum liquid flow considerations discussed in the Appendix, which do not suffer many of the approximations of the analysis, show a forbidden zone in this region where drops cannot be formed.

Whereas this analysis of the drop formation problem shows a number of properties not indicated by other approximate considerations, some known properties of such drop formation are not predicted. The linear treatment does not predict the formation of satellite droplets. And again, the alteration of the average stream velocity and the forbidden zone of drop formation, as discussed in the Appendix, are not predicted by this linear theory.

The formation of satellite droplets is shown in Lee's work [3] in which he used the one-dimensional analysis with a spatially periodic perturbation. He dealt numerically with the nonlinear differential equations. His work, however, always predicts the formation of satellite droplets. Experimentally, it is known that there are regions of the perturbation where no satellite formation exists and other regions where such satellite formation is aggravated. The author believes that the key to this problem lies in the dispersive nature of the medium. The nonlinear theory would cause an initially sinusoidal perturbation to develop into a wave including the harmonic frequencies. Unstably growing waves of these different frequencies would form a beat frequency envelope on the stream. The exact shape and form of drop formation would depend on how the beat frequency envelope matches the traveling waves at the drop separation point. The formation of satellite droplets would be either suppressed or enhanced by this interaction. A nonlinear treatment of the boundary value analysis would show the plausibility of this hypothesis.

Acknowledgments

The author acknowledges the help given him by H. C. Lee through many discussions. He is also indebted to J. S. Lew for his review of an initial draft and his analytical solution to the matrix equation.

Appendix: Forbidden drop formation zone

As drops are formed, the average velocity of the liquid decreases. This phenomenon, which is not predicted by the linear analysis that is the subject of this paper, is most important at the lower jet velocities. Thus we include this Appendix, which is a digression from the subject of the paper, for the purpose of investigating this effect.

The considerations used in this section involve the gross momentum balance and liquid flow rate conservation of the jet. The many assumptions and approximations made in the analysis in the main body of this paper, therefore, do not apply to this section. The only assumptions made are that the jet starts with a flat velocity profile and ends as independent drops. The liquid at both ends is relaxed, and effects of air interaction and gravity are ignored.

Schnieder, Lindblad, Hendricks, and Crowley [9] looked at this effect, in which the liquid velocity changes. The author, however, disagrees with their analysis and results, hence the necessity to consider the effect again. This paper considered the situation by analyzing the momentum relationships that exist in this steady state phenomenon. For this consideration, construct an imaginary box around the whole drop formation zone, so that only the unperturbed stream enters the box on one side with a flat plug-type velocity profile, and spherical drops emanate from the other side. It matters not whether viscous forces exist within the box or whether satellite drops are formed, as long as they recombine to make spherical drops inside the box, because all such forces would be internal to the momentum system. The momentum flow into the box minus the momentum flow from the box would equal the external forces that exist at the boundaries of this imaginary box.

Schneider, et al. [9], presented the analysis. However, in the calculation of the external forces on the boundaries of the imaginary box, they considered only the surface tension forces. They neglected to include the internal pressure of the stream, i.e., the pressure that is a result of surface tension. When both forces are included in the analysis, we obtain

$$\frac{v_{\rm D}}{v_{\rm o}} = \left(1 - \frac{v_{\rm c}^2}{v_{\rm o}^2}\right) = (1 - 2\epsilon^2),\tag{A1}$$

where v_0 is the original stream velocity, $v_{\rm D}$ is the final drop velocity, $v_{\rm c}$ is the capillary velocity as defined in Eq. (14), and ϵ^2 is defined by Eq. (13).

For values of the jet velocity equal to or less than the capillary velocity ($\epsilon^2 \ge 0.5$), the drop velocity perishes. In other words, there is no drop formation; also there is no stream. The momentum flow from a nozzle must be great enough to overcome the negative force on the ejected stream, otherwise the stream cannot be ejected as a steady stream.

Smith and Moss [10] and others [11, 12] long ago noted that a certain pressure was necessary before a steady stream could be emitted from a nozzle. They spoke of a "critical velocity" that was given by an equation almost identical with the expression for capillary velocity.

A second effect must be addressed before the forbidden drop formation zone can be delineated: There has to be enough room in the stream for the formed drops. If the wavelength is very short compared to the stream diameter, a segment of the original stream, which would eventually become an individual drop, would have a pillbox shape with its diameter being much greater than its thickness (the wavelength). The diameter of the drop that would contain the same volume would be larger than the pillbox thickness; therefore, steady state drop

155

formation would be impossible. The wavelength for which the drop diameter would just equal the wavelength is given by

$$\frac{\pi d^2 \lambda}{4} = \frac{\pi}{6} \,\lambda^3,\tag{A2}$$

which yields

$$\frac{\lambda}{d} = \sqrt{1.5} = 1.2247;$$
 (A3)

$$\omega^2 = 6.5819$$
.

Therefore, drop formation for wavelengths less than 1.2247 diameters of the stream is impossible.

The wavelength that is of importance in this consideration is the wavelength at drop formation. Because of the decrease in liquid velocity, Eq. (A1), the wavelength of the original stream is larger; from Eq. (A1), we get

$$\frac{d^2\lambda_0}{4} = \frac{\lambda_D^3}{6} \tag{A5}$$

01

$$\omega^2 = \frac{\pi^2}{1.5} (1 - 2\epsilon^2)^3. \tag{A6}$$

The dotted line in Fig. 1 shows the line given by Eq. (A6). For the region above and to the right of this line, there is not enough room for the drops to form.

One might ask: What happens to a jet in this forbidden zone? If the momentum flow rate is not great enough

 $(\epsilon^2 > 0.5)$, the nozzle would drip profusely if placed in a gravitational field. For $\epsilon^2 < 0.5$, presumably the stream would break up into drops as a stream that was not purposefully perturbed; that is, a jet that was subject to only "white noise" vibration.

References

- Lord Rayleigh, "On the Instability of Jets," Proc. London Math. Soc. X (1878).
- 2. Lord Rayleigh, Scientific Papers, Cambridge University Press, London, 1899, Vol. 1, p. 361.
- H. C. Lee, "Drop Formation in a Liquid Jet," *IBM J. Res. Develop.* 18, 364 (1974).
- 4. V. I. Levich, *Physicochemical Hydrodynamics*, Prentice-Hall Inc., Englewood Cliffs, N.J., 1962, p. 361.
- J. B. Keller, S. I. Rubinow, and Y. O. Tu, "Spatial Instability of a Jet." *Physics of Fluids* 16, 2052 (1973).
- 6. H. Portig, private communication.
- 7. J. S. Lew, private communication.
- 8. E. W. Cheney, Introduction to Approximation Theory, McGraw-Hill Book Company Inc., New York, 1966.
- J. M. Schnieder, N. R. Landblad, C. D. Hendricks, and J. M. Crowley, J. App. Phys. 38, 2599 (1967).
- S. W. J. Smith and H. Moss, "Experiments with Mercury Jets," Proc. Roy. Soc. A93, 373 (1917).
- E. Tyler and E. G. Richardson, "The Characteristic Curves of Liquid Jets," Proc. Phys. Soc. 37, 297 (1925).
- A. C. Merrington and E. G. Richardson, "The Break-up of Liquid Jets," *Proc. Phys. Soc.* 59, 1 (1947).

Received March 24, 1975; Revised June 27, 1975

The author is located at the IBM System Communications Division laboratory, Endicott, N.Y. 13760.